ICAS-98-4,1,3

A98-31578

SIMULATION OF HELICOPTER FLIGHT DYNAMICS AFTER TAIL ROTOR LOSS OR MAIN ROTOR BLADE FAILURE

Olympio A. F. Mello*
Instituto de Aeronáutica e Espaço
Centro Técnico Aeroespacial
12228-904 - São José dos Campos - SP
Brazil

Abstract

Two applications of flight simulation to the investigation of helicopter accidents are presented. In the first, an accident with typical tail rotor loss characteristics is considered. The investigation board worked on two hypotheses, namely tail rotor shaft failure and pilot's loss of pedal control after he suddenly increased the collective pitch near the ground and delayed applying pedals as needed. A simulation was conducted using simple models of yaw dynamics and tail rotor aerodynamics, and results indicated that pedal control would still be available even with a three second pilot delay in applying the pedals, therefore the hypothesis of loss of pedal control was discarded. In the second application, a helicopter accident at sea in which the aircraft wreck had not been recovered is considered. In that case, the investigation board had to rely on information from the Cockpit Voice/Flight Data Recorder (CVFDR) and a video recorded by an undersea robot. The most significant information obtained from the FDR were extremely high vibrations in all three axes, at a frequency associated with the first harmonic of main rotor rotational speed. The investigation was directed towards several hypotheses associated with main rotor blade and assemblies that might explain the vibrations. A simulation program based on an existing general helicopter flight simulation code was developed and simulations were conducted for the assumed blade failure hypotheses. Results indicated that the excessive accelerations were consistent with the loss of a large rotating mass, due to blade fracture near the root. In both applications, simulation provided substantial grounds for the investigation boards to establish the most probable causes for the accidents.

Introduction

When investigating helicopter accidents — or any aeronautical accident — it is not unusual to come to questions that can only be answered by flight simulation. However, in many cases these simulations are not straightforward, as simulation programs are not often developed with the capability to simulate failure hypotheses, which may vary widely.

In this paper, two examples of application of simulation programs to the investigation of helicopter accidents are presented. In the first case, an accident with typical tail rotor loss characteristics occurred, but the tail rotor blades left marks on the ground which suggested that the tail rotor was still spinning. This evidence raised an alternate possibility that the accident might have occurred due to the pilot's delay in applying pedals during the flare maneuver. In order to investigate both hypotheses, a very simple model was developed to simulate yaw dynamics and tail rotor rotational speed decrease after tail rotor shaft failure.

In the second application, a helicopter had crashed on the sea surface after suffering excessive vibrations. Only the flight data and cockpit voice recorders were retrieved, and the investigators had to rely on simulation to establish possible causes for the accident. For this investigation, a more detailed simulation code, based on an existing program, was developed in order to simulate several hypotheses associated with failures in the main rotor blades and assemblies.

Tail Rotor Loss

After a helicopter accident† with typical tail rotor loss characteristics, it was suggested that the accident might have occurred due to pilot's loss of pedal control after he suddenly increased the collective pitch near the ground and delayed applying pedals as needed. This possibility was apparently supported by marks left on the ground indicating that the tail rotor was still spinning when it hit the ground. The investigation board established two working hypotheses, namely loss of pedal control due to excessive pilot delay and loss of tail rotor due to shaft failure.

*Senior Research Engineer, Space Systems Division

†Specific accident details, such as date and aircraft, are not given in order to preserve investigation confidentiality.

In order to investigate the first hypothesis, a numerical simulation of aircraft yaw dynamics without loss of tail rotor rotational speed was performed. In order to investigate the second hypothesis, a numerical simulation of aircraft yaw dynamics coupled with tail rotor blade rotation dynamics was performed. In both cases, the helicopter was assumed trimmed in hover with main rotor torque at 45%. The sudden increase in collective pitch was modeled by a corresponding sudden increase in main rotor torque from 45% to 95%, applied during a one second ramp, after which the torque remained constant at 95%. For the second hypothesis, it was assumed that shaft failure occurred at the same time the increase in collective pitch started.

For the simulation of both hypotheses, simple models of the aircraft yaw dynamics and tail rotor aerodynamics were used. In the tail rotor loss case, a model for blade rotation dynamics was also used. These models will be discussed next.

Simulation Model

The yaw equation of motion was obtained by considering main rotor torque, aircraft yaw inertia, tail rotor thrust and vertical empennage drag. Fig. 1 illustrates the conventions used here.

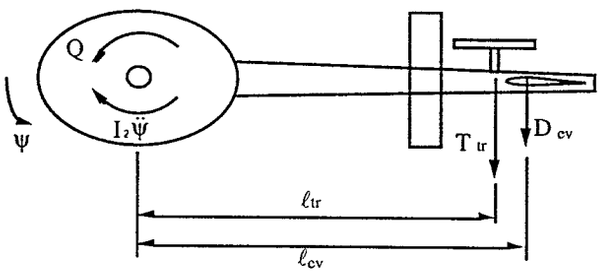

Figure 1: Contributing Forces and Moments for Yaw Dynamics

The governing equation for yaw dynamics used here is:

$$Q_{\mathrm{mr}} - I_z\ddot{\psi} - T_{\mathrm{tr}}\ell_{\mathrm{tr}} - D_{\mathrm{ev}}\ell_{\mathrm{ev}} = 0 \qquad (1)$$

where $Q_{\mathrm{mr}} = Q_{\mathrm{mr}}(t)$ is the main rotor torque, I_z is the helicopter yaw moment of inertia with respect to the main rotor axis, ψ is the yaw angle, $T_{\mathrm{tr}} = T_{\mathrm{tr}}\left(\dot{\psi}\right)$ is the tail rotor thrust, ℓ_{tr} is the distance between the main and tail rotor axes, $D_{\mathrm{ev}} = D_{\mathrm{ev}}\left(\dot{\psi}\right)$ is the vertical empennage drag and ℓ_{ev} is the distance between the vertical empennage center of pressure and the main rotor axis. Note that, in the above equation, fuselage drag has been neglected, as the main contribution in terms of yaw moment is due to the vertical empennage drag.

As mentioned above, the helicopter was assumed initially trimmed in hover with main rotor torque at 45%. The sudden increase in collective pitch was modeled by a corresponding sudden increase in main rotor torque from 45% to 95%, applied during a one second ramp, after which the torque remained constant at 95%.

If the pilot increases collective pitch without adjusting the pedals accordingly, the helicopter enters yaw motion due to low tail rotor thrust. In this condition, the tail rotor operates in a way similar to a main rotor in descent. The treatment presented here uses this analogy. An equivalent "vertical" rotor velocity (positive when rotor is climbing) due to the yaw movement is $V = -\ell_{\mathrm{tr}}\dot{\psi}$.

The tail rotor operating regime in this equivalent descent depends on this equivalent "vertical" velocity. It may be normal operating state, vortex ring/turbulent wake state or windmill brake state[1]. The state in which the tail rotor operates may be established from the ratio V/v_h, where v_h is the induced velocity in "hover", which corresponds here to the induced velocity for zero yaw speed, given by:

$$v_h = \Omega_{\mathrm{tr}} R_{\mathrm{tr}} \sqrt{\frac{C_{T_{\mathrm{tr}}}}{2}} \qquad (2)$$

where Ω_{tr} is the tail rotor angular velocity, R_{tr} is the tail rotor radius and $C_{T_{\mathrm{tr}}}$ is the tail rotor thrust coefficient. The tail rotor operating state is established as follows:

(a) if $V/v_h \geq -1$, normal operating state;

(b) if $-2 < V/v_h < -1$, vortex ring/ turbulent wake state;

(c) if $V/v_h \leq -2$, windmill brake state.

For all tail rotor operating states, a blade element approach is used. The blade is divided into sections (elements), for which aerodynamic forces are calculated and summed up to yield tail rotor thrust and thrust coefficient. In order to compute lift and drag coefficients, the induced velocity v_i at a given section is needed. The computation of this velocity has to be performed in a specific manner for each operating state. For normal operating state, combined momentum and blade element theories give:

$$\lambda = \left(\frac{\lambda_c}{2} - \frac{\sigma a}{16}\right) + \sqrt{\left(\frac{\lambda_c}{2} - \frac{\sigma a}{16}\right)^2 + \frac{\sigma a \theta_{\mathrm{tr}} r}{8}} \qquad (3)$$

where $\lambda = (V + v_i)/\Omega_{\mathrm{tr}} R_{\mathrm{tr}}$ is the total inflow ratio, $\lambda_c = V/\Omega_{\mathrm{tr}} R_{\mathrm{tr}}$ is the climb inflow ratio, $\sigma = N_{b_{\mathrm{tr}}} c_{\mathrm{tr}}/\pi R_{\mathrm{tr}}$ is the solidity ratio, a is the mean blade section lift curve slope, $N_{b_{\mathrm{tr}}}$ is the number of blades, c_{tr} is the chord, θ_{tr} is the pitch angle and r is the section radial location. From Eqn. (3) and the definition of λ, v_i may be obtained:

$$v_i = \lambda_i \Omega_{\rm tr} R_{\rm tr} = (\lambda - \lambda_c)\,\Omega_{\rm tr} R_{\rm tr} \qquad (4)$$

where λ_i is the induced inflow ratio. For vortex ring/turbulent wake state, no theory yields a simple expression for the mean induced velocity. Therefore, the following empirical formula[2] is used:

$$v_i = v_h \left(\frac{V}{v_h}\right)\left[0.373\left(\frac{V}{v_h}\right)^2 - 1.991\right] \qquad (5)$$

For windmill break state, momentum theory gives the mean induced velocity as:

$$v_i = -\frac{V}{2} - \sqrt{\left(\frac{V}{2}\right)^2 - v_h^2} \qquad (6)$$

Once the induced velocity is computed using either Eqns. (4), (5) or (6), depending on the tail rotor operating state, one may obtain the induced angle at a given element $\phi = \tan^{-1}(U_P/U_T)$, where $U_P = V + v_i$ is the velocity normal to the blade and $U_T = \Omega_{\rm tr} r$ is the velocity tangential to the blade. The blade effective angle of attack is then given by $\alpha = \theta_{\rm tr} - \phi$.

Section lift (c_ℓ) and drag (c_d) coefficients are obtained from experimental data[3]. From these coefficients, blade element lift, drag and the resulting contribution to normal force may be computed:

$$dF_z = (c_\ell \cos\phi - c_d \sin\phi)\,\frac{\rho U^2 c_{\rm tr}}{2} dr \qquad (7)$$

where $U = \sqrt{U_T^2 + U_P^2}$ is the total blade section velocity and ρ is the air density. Integration of these contributions along the blade gives the total blade normal force and consequently tail rotor thrust and thrust coefficient:

$$T_{\rm tr} = N_b F_z = N_b \int_{r_{i_{\rm tr}}}^{R_{\rm tr}} dF_z \qquad (8)$$

$$C_{T_{\rm tr}} = \frac{T_{\rm tr}}{\rho \pi R_{\rm tr}^2 \left(\Omega_{\rm tr} R_{\rm tr}\right)^2} \qquad (9)$$

where $r_{i_{\rm tr}}$ is the blade root cut-out.

In the computation of tail rotor thrust, the blade pitch is required. The pitch is set by the pilot pedal control. Here, it is assumed that the helicopter is initially at trim in hover, with the pedal adjusted to compensate for main rotor torque at 45%, as described previously. In this investigation, the pilot is assumed to have delayed applying the pedals for a time t_θ. After this delay, the pitch would be increased from the initial value $\theta_{\rm tr_0}$ to the maximum pitch $\theta_{\rm tr_{max}}$, during a one second ramp, after which the pitch remained constant.

The initial and maximum pitch are determined from the tail rotor thrust which is needed to compensate the initial torque $Q_{\rm mr_0} = Q_{\rm mr_{45\%}}$ and the maximum torque $Q_{\rm mr_{max}}$, respectively. The thrust needed to compensate a given torque $Q_{\rm mr}$ is $T_{\rm tr} = Q_{\rm mr}/\ell_{\rm tr}$ and the thrust coefficient corresponding to this thrust is computed from the definition of C_T, Eqn. (9). The tail rotor pitch is found from the following expression, derived from combined blade element and momentum theories[2]:

$$\theta_{\rm tr} = \frac{6 C_{T_{\rm tr}}}{\sigma a} + \frac{3}{2}\sqrt{\frac{C_{T_{\rm tr}}}{2}} \qquad (10)$$

For the purposes of this investigation, the vertical empennage is represented by a plate in stagnation flow. The vertical drag is therefore given by:

$$D_{\rm ev} = \frac{1}{2}\rho V_{\rm ev}^2 A_{\rm ev} c_{D_{\rm ev}} \qquad (11)$$

where $V_{\rm ev}$ is the velocity normal to the empennage, $A_{\rm ev}$ is the vertical empennage area and $c_{D_{\rm ev}}$ is the plate drag coefficient, estimated to be 1.2[4].

For tail rotor loss simulations, the blade rotational equation of motion is also needed. Neglecting transmission and shaft friction, the contributing moments are blade inertia and tail rotor torque due to aerodynamic forces. Thus the equation for tail rotor angular velocity $\Omega_{\rm tr}$ is:

$$I_{b_{\rm tr}} \dot{\Omega}_{\rm tr} + Q_{\rm tr} = 0 \qquad (12)$$

where $I_{b_{\rm tr}}$ is the blade moment of inertia with respect to the tail rotor axis and $Q_{\rm tr}$ is the tail rotor torque, obtained from integration of blade element contributions:

$$Q_{\rm tr} = N_b \int_0^{R_{\rm tr}} (c_d \cos\phi + c_\ell \sin\phi)\,\frac{\rho U^2 c_{\rm tr}}{2} r dr \qquad (13)$$

For simulations without loss of tail rotor rotational speed, Eqn. (1) is integrated in time using a standard fourth-order Runge-Kutta scheme[5]. For simulations with loss of rotational speed, both Eqns. (1) and (12) are integrated simultaneously using the same scheme.

Simulation Results

The simulated yaw motion for the hypothesis of constant tail rotor rotational speed, i.e., no shaft failure, is presented in Figure 2. In this figure, three simulations are shown. The first two correspond to pilot delays of 2 and 3 seconds, respectively, in applying the pedals after collective pitch increase. In these simulations, pedals were applied in a one-second ramp. The third simulation corresponds to no pilot pedal adjustment after collective pitch increase. It is clear from these simulations that even after a three-second delay the pilot is able to adjust the aircraft heading before making a complete turn. Actual pilot delays depend on the disturbance[6] and typically do not exceed 0.25 sec.[7, 8]. Actual time required to apply full controls would take well less than one second[8, 9]. The pilot

delays assumed here are much higher than what might be expected and therefore the hypothesis of loss of directional control due to pilot delay is discarded.

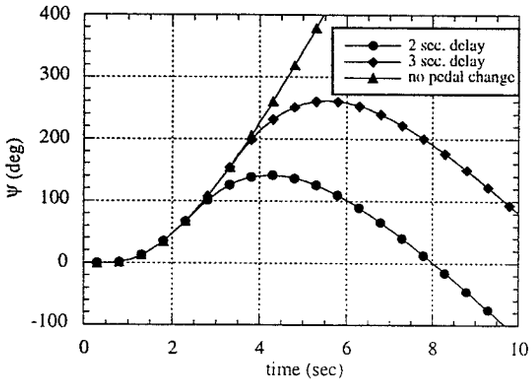

Figure 2: Yaw Motion without Loss of Tail Rotor

The simulated yaw motion for the hypothesis of loss of tail rotor rotational speed due to shaft failure is presented in Figure 3. In this figure, three simulations are shown. The first corresponds to a pilot delay of 2 seconds in applying the pedals after collective pitch increase. The second simulation corresponds to no pilot pedal adjustment after collective pitch increase. The third simulation corresponds to no collective pitch increase or pedal change. Tail rotor rotational speeds for these simulations are presented in Figure 4.

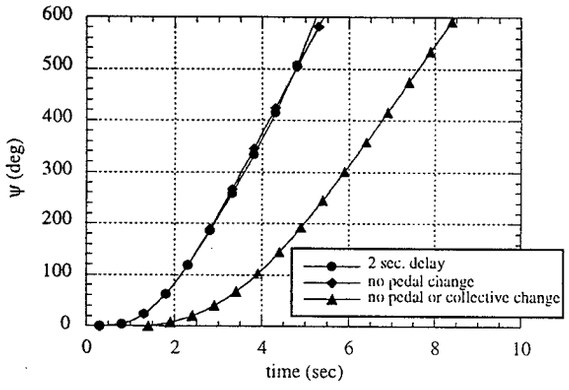

Figure 3: Yaw Motion after Tail Rotor Shaft Failure

From these simulations, it is seen that shaft failure quickly causes loss of directional control, as expected. However, if the pedals are not applied the rotational speed eventually reaches a constant value, as the tail rotor enters an autorotative regime in vortex ring/turbulent wake state. If pedals are fully applied, the tail rotor enters windmill brake state and the rotational speed decreases. This implies that the rotational speed on impact depends on when and to what extent the pedals are applied. Therefore, even with loss of tail rotor shaft, it would be possible for the tail rotor to hit the ground at a range of rotational

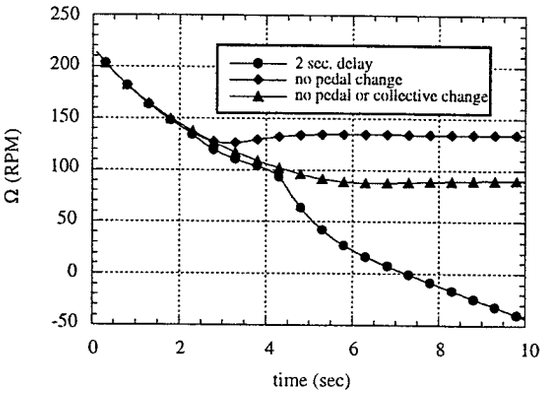

Figure 4: Tail Rotor Rotational Speed after Tail Rotor Shaft Failure

speeds which could account for the marks left on the ground. This result provided the investigators with evidence to support the hypothesis of tail rotor shaft failure.

Main Rotor Blade Failure

In this accident, a helicopter[‡] was on its way to an offshore oil rig. A sudden bang was heard, the aircraft started suffering from excessive vibrations and the crew lost control of the aircraft, which crashed on the sea surface.

An initial attempt to retrieve the wreck was unsuccessful, but the combined Flight Data Recorder (FDR) / Cockpit Voice Recorder (CVR) was recovered. A video showing the wreck was recorded by an undersea robot.

Although some channels were apparently defective, among those the lateral cyclic position, the FDR proved to be an essential contribution to this particular investigation. Most significant were the extremely high vibrations in all three axes, most notably a ± 1 g longitudinal vibration and a ± 0.4 g lateral vibration.

Spectral analysis of the FDR acceleration data is shown in Figure 5. From this figure, normal vibrations appear to be associated with a 3.6 Hz frequency, very close to the main rotor rotational speed (3.43 Hz in this case). Longitudinal and lateral vibrations appear to be associated with a 0.4 Hz frequency. However, while the normal accelerations were sampled at 8 Hz, which allows identification of frequencies up to 4 Hz, longitudinal and lateral accelerations were sampled at 4 Hz, which allows spectral analysis up to 2 Hz only. For this reason, the signal was aliased and the peak at 0.4 Hz actually represents phenomena associated with the difference 4 Hz - 0.4 Hz = 3.6 Hz, which is the same frequency identified by spectral analysis of the normal accelerations.

[‡]Specific accident details, such as date and aircraft, are not given in order to preserve investigation confidentiality.

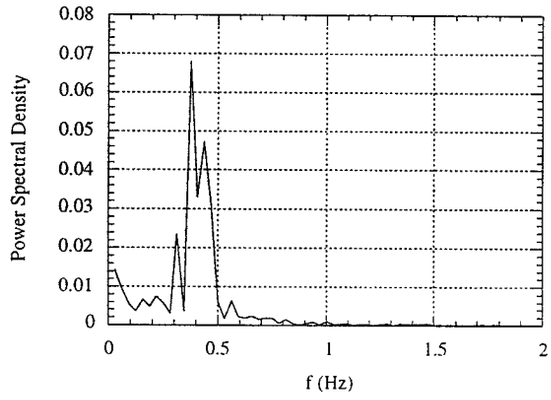

(a) Longitudinal acceleration

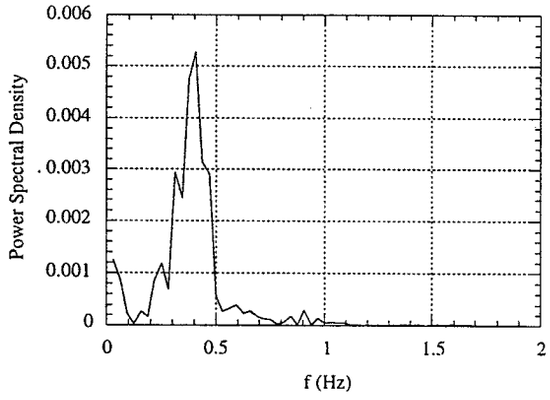

(b) Lateral acceleration

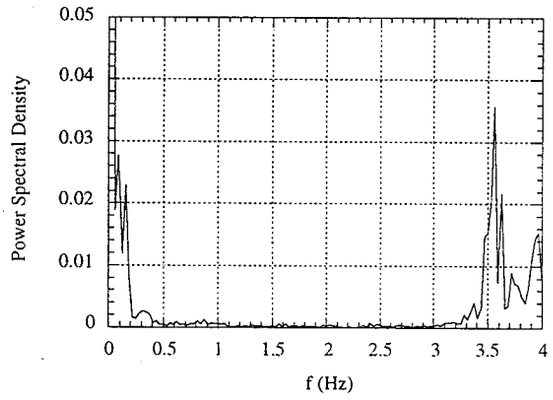

(c) Normal acceleration

Figure 5: Power Spectral Density of FDR-recorded Accelerations

From these considerations, it was found that the vibrations were associated with the first harmonic of main rotor rotational speed.

As mentioned before, the aircraft wreck had not been recovered for rotor head and blade material analysis. However, the undersea video allowed the investigators to identify some possible failure hypotheses, all related with main rotor blades and assemblies. These hypotheses were:

1. Total loss of one blade;
2. Blade spar fractured near the root;
3. Blade spar fractured near the tip;
4. Loss of balancing block near the tip
5. Loss of portions of some blade sections aft of the spar (trailing edge pockets);
6. Loss of one lag damper;
7. Loss of one pitch link;
8. Damaged pitch link, resulting in excessive slack.

Simulation Methodology

Since the aircraft wreck was not available for analysis, simulation of the failure hypotheses was essential in the determination of the most probable cause. The helicopter manufacturer conducted their own simulations of hypotheses nos. 3, 6 and 7 using an aeroelastic code not coupled with flight dynamics. These simulations pointed to hypothesis no. 3 as the most probable. However, the vibration levels resulting from the simulations were still substantially lower than the levels recorded by the FDR. The manufacturer suggested that this might be due to the absence of aircraft motion in the simulation.

In order to provide a more consistent basis for determination of the most probable cause, a simulation program based on an existing general helicopter flight simulation code[10] was developed. In this method, the aircraft has six degrees of freedom and the rotor blades have three rigid body degrees of freedom — flapping, lagging and pitching. A blade element method is used, in which the aerodynamic coefficients are computed from simple algebraic equations based on experimental airfoil data. A first-order dynamic inflow model[11] is incorporated for computation of rotor wake downwash[12]. Section forces are integrated along the blade and summed up to yield main rotor forces and moments. These are added to fuselage, tail rotor and vertical and horizontal stabilizer forces and moments, so that total aircraft forces and moments can be obtained. From these, aircraft accelerations are found and integration of the equations of motion is performed. Details of the basic simulation method

are available in Ref. [10] and therefore are not presented here.

Simulation of blade failure hypotheses is conducted by appropriate modification of blade force computation. For the simulations presented here, the helicopter is initially trimmed. After a specified time (0.25 sec.), one of the failure hypotheses under investigation is introduced, as follows:

- Loss of blade or portion of the blade (hypotheses 1 to 4): Contributions of lost sections to blade inertial and aerodynamic forces are eliminated;
- Loss of trailing edge pockets (hypothesis 5): Contribution of lost parts to blade inertial forces are eliminated; aerodynamic coefficients of affected sections are modified to represent reduction in lift — assumed 30% — and increase in drag — assumed 100%;
- Loss of one lag damper (hypothesis 6): Force due to lag damper is eliminated;
- Loss of pitch link or slack (hypotheses 7 and 8): The pitch link is modeled by a torsional spring[2]; when it fails the moment due to this spring is eliminated. If there is some slack, the spring is effective only when the difference between the control pitch and the actual pitch is greater than the specified slack.

Simulations were conducted for all the above hypotheses in three modes: In the first, the helicopter was not allowed to move. This case was simulated so that the results could be compared with the simulations conducted by the manufacturer. In the second mode, the helicopter was allowed to move freely in space, with the controls held fixed to the trim positions. In the third mode, the helicopter was free to move, but the control positions were input during the simulation according to the positions registered in the FDR, except for the lateral cyclic, for which the FDR register was inoperative.

Simulation Results

A substantial amount of results was generated in this investigation, since eight failure hypotheses and three simulation modes were considered. Only some representative results are shown here.

Simulated and registered accelerations for hypothesis no. 2 (blade fractured near the root) for the free aircraft, pilot-in-the-loop simulation mode, are shown in Figure 6. Results for hypothesis no. 1 (total blade loss) are very similar and are not shown for brevity. From these results, it may be seen that these hypotheses would cause vibrations consistent with the FDR data. It should be recalled that the flight-recorded

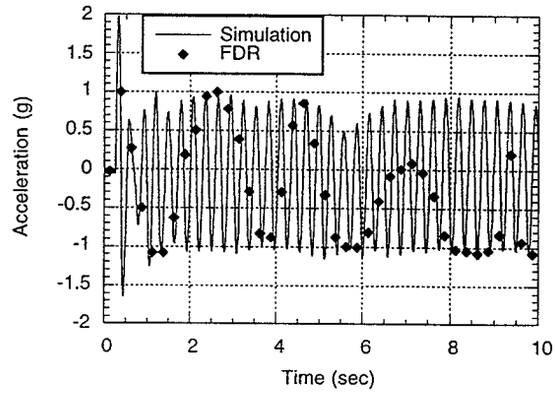

(a) Longitudinal accelerations

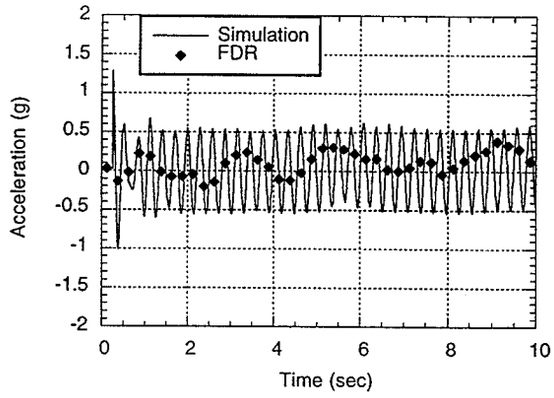

(b) Lateral accelerations

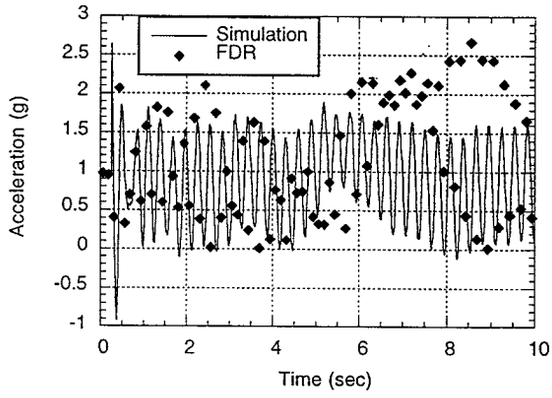

(c) Normal accelerations

Figure 6: Simulated and registered accelerations for hypothesis no. 2 (blade fractured near the root), pilot in the loop.

data were sampled at a frequency lower than the rotational frequency, hence the noticeable aliasing.

Simulated and registered accelerations for hypotheses nos. 3 (blade fractured near the tip), 6 (loss of lag damper) and 7 (loss of one pitch link) for the free aircraft, pilot-in-the-loop simulation mode, are shown in Figures 7 through 9, respectively. It may be seen that these hypotheses would cause significantly lower vibrations than recorded. The other hypotheses under investigation — for which the results are not shown here — cause even lower vibrations.

In order to illustrate in what extent aircraft motion induced higher levels of acceleration, simulated and registered accelerations for hypothesis no. 2, fixed aircraft, pilot-out-of-the-loop simulation mode are presented in Figure 10. By comparison between this Figure and Figure 6, it may be seen that introduction of aircraft motion affects significantly only normal accelerations, while longitudinal and lateral accelerations are not affected much. Therefore, a fixed-aircraft simulation could still provide a good indication of probable causes for this accident.

Although the unavailability of lateral cyclic register in the FDR was a serious handicap in the pilot-in-the-loop simulations, acceleration levels were quite consistent with those recorded. However, aircraft attitude could not be correctly simulated. This is illustrated in Figure 11, where aircraft pitch attitude as simulated for hypothesis no. 2, pilot-in-the-loop mode, is compared with FDR-registered attitudes. This was due to the fact that the lateral cyclic was held constant during these simulations. Nevertheless, the trends in aircraft response are consistent. Since aircraft motion was found not to affect substantially longitudinal and lateral accelerations, these discrepancies are not relevant with respect to characterization of vibration levels for the different hypotheses considered here.

Overall, these results indicated that the excessive accelerations were consistent with the loss of a large rotating mass, as in hypotheses nos. 1 and 2. Therefore, the simulation provided substantial grounds for the investigation board to establish these hypotheses as the most probable causes and to discard the other hypotheses.

Concluding Remarks

Two applications of flight simulation to the investigation of helicopter accidents were presented. In the first application, simulations of yaw dynamics with and without tail rotor loss were carried out in order to determine if loss of pedal control due to pilot's delay could be the cause of an accident with loss of directional control, and if the tail rotor could still be spinning when it hit the ground in case of tail rotor shaft failure. The results indicated that pedal control would still be available even with a three second pilot delay in applying the pedals, therefore the hypothesis

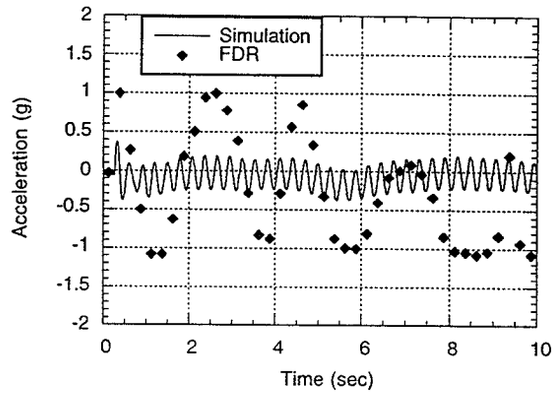

(a) Longitudinal accelerations

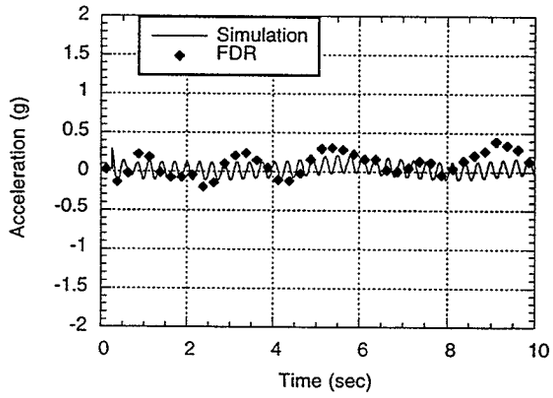

(b) Lateral accelerations

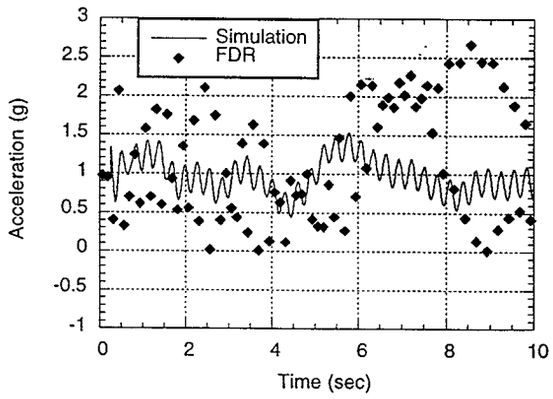

(c) Normal accelerations

Figure 7: Simulated and registered accelerations for hypothesis no. 3 (blade fractured near the tip), pilot in the loop.

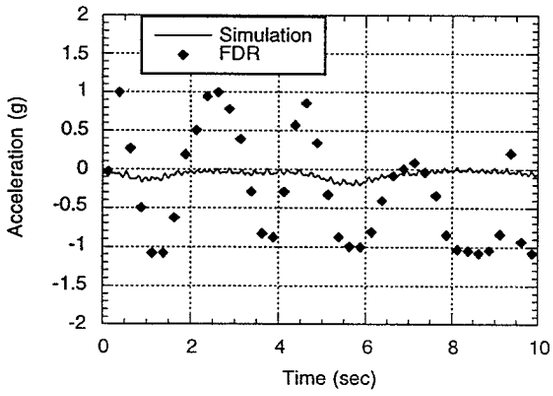

(a) Longitudinal accelerations

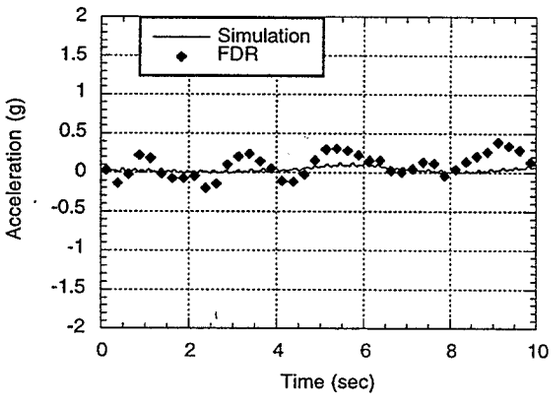

(b) Lateral accelerations

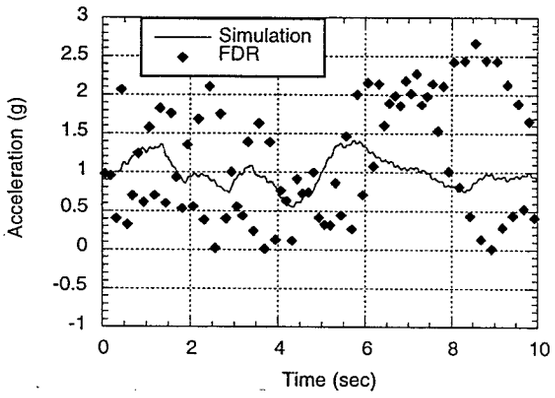

(c) Normal accelerations

Figure 8: Simulated and registered accelerations for hypothesis no. 6 (loss of one lag damper), pilot in the loop.

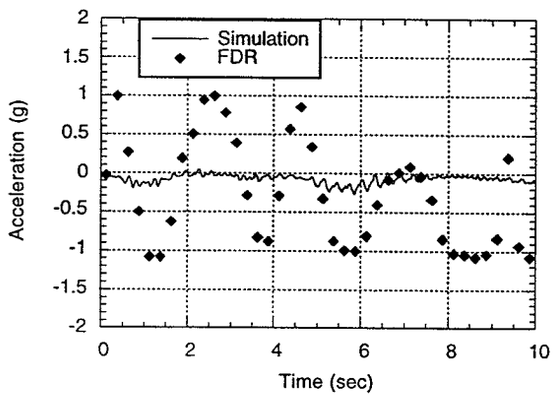

(a) Longitudinal accelerations

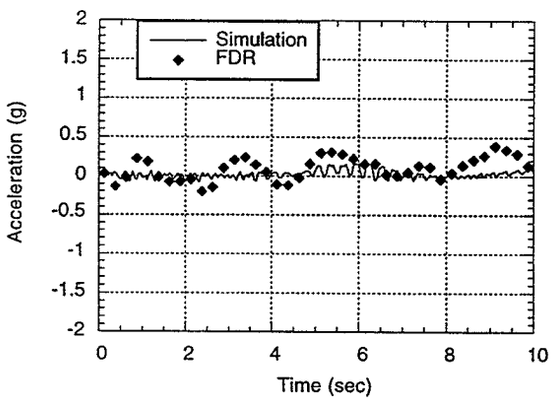

(b) Lateral accelerations

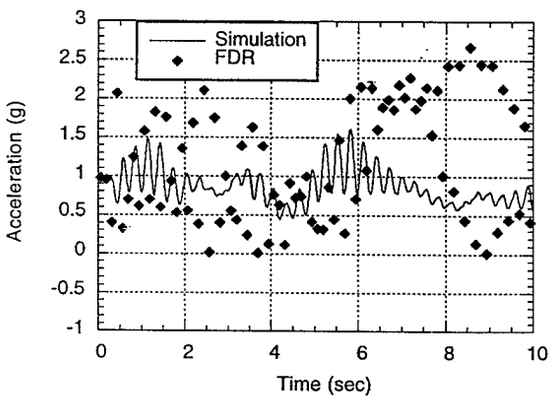

(c) Normal accelerations

Figure 9: Simulated and registered accelerations for hypothesis no. 7 (loss of one pitch link), pilot in the loop.

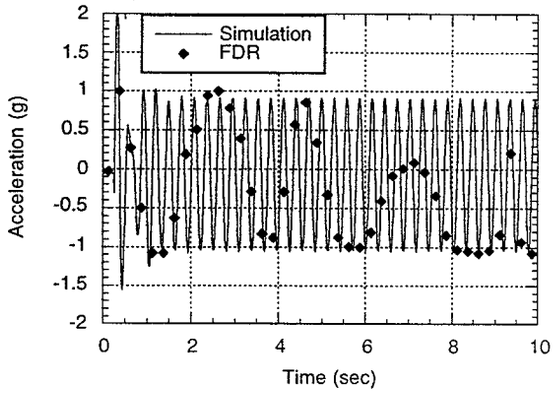

(a) Longitudinal accelerations

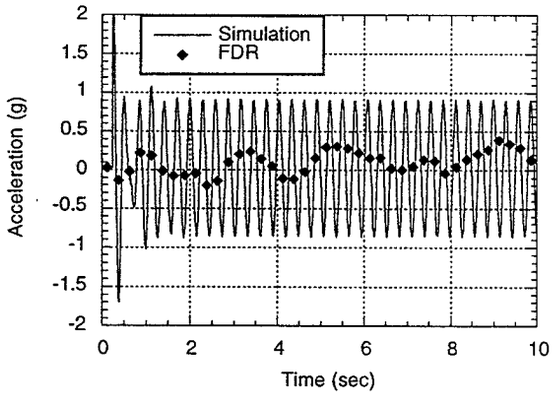

(b) Lateral accelerations

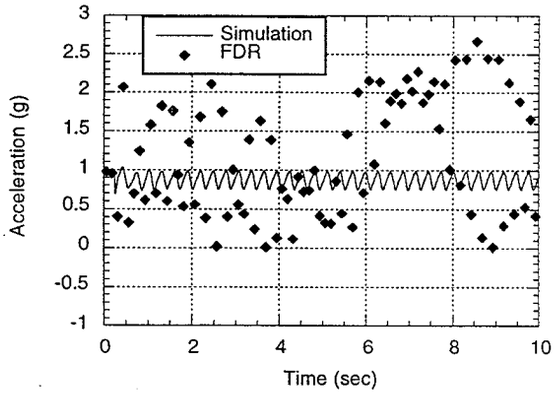

(c) Normal accelerations

Figure 10: Simulated and registered accelerations for hypothesis no. 2 (blade fractured near the root), pilot out of the loop, aircraft fixed in space.

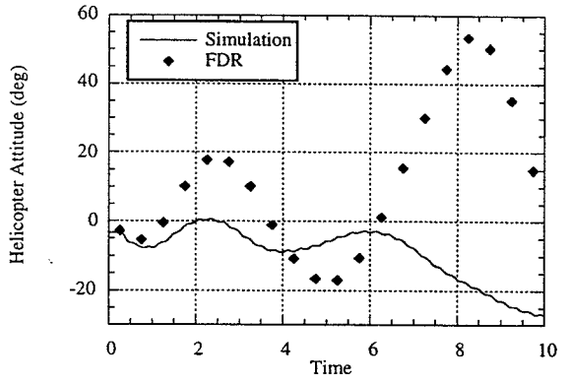

Figure 11: Simulated and registered aircraft attitudes for hypothesis no. 2 (blade fractured near the root), pilot in the loop

of loss of pedal control was discarded. The simulation also indicated that the rotor blade could have hit the ground within a range of rotational speeds after tail rotor shaft failure, which could account for the marks on the ground, therefore maintaining the hypothesis of tail rotor loss.

In the second application, a numerical simulation of helicopter flight after several blade failure hypotheses has been conducted. Because in that case the aircraft wreck had not been recovered, simulation was essential to the investigation board in establishing the most probable cause of the accident. Simulations were conducted with and without the pilot in the loop, and for the latter, with and without aircraft movement in space. Longitudinal and lateral acceleration levels for these different simulation modes did not differ substantially, therefore simulation without aircraft movement or pilot control was sufficient for characterization of the effects of blade failure. Simulated accelerations indicated that the excessive accelerations were consistent with the loss of a large rotating mass, either due to total blade loss or blade fracture near the root. Simulated aircraft attitude changes did not compare well with FDR-recorded data, probably due to the unavailability of lateral cyclic positions.

In both applications, the simulations conducted here allowed clear characterization of the hypotheses under investigation, therefore the goal of providing the investigators with substantial grounds for establishing the most probable causes was attained.

References

1. Gessow, A., & Myers, G. C., Jr., *Aerodynamics of the Helicopter*, Frederick Ungar, 1952. Reprint, College Park Press, College Park, MD, 1985.

2. Johnson, W., *Helicopter Theory*, Princeton University Press, Princeton, New Jersey, 1980.

3. Sadler, S. G., "Main Rotor Free Wake Geometry Effects on Blade Air Loads and Response for Helicopters in Steady Maneuvers; Vol. I: Theoretical Formulation and Analysis of Results," NASA CR-2110, Washington, DC, 1972.

4. ESDU - Engineering Sciences Data Unit, "Fluid Forces, Pressures and Moments on Rectangular Blocks," In: "ESDU Aeronautical Series, Aerodynamic Sub-Series, Vol. 4b - Aerodynamics of Bodies, Controls and Flaps," Item No. 71016, with Amendments A to C, Engineering Sciences Data Unit, London, 1978.

5. Beyer, W. H., ed., *CRC Standard Mathematical Tables,* 28th ed., CRC, Boca Raton, Florida, 1987.

6. Kuehnel, H. A., "In-Flight Measurement of the Time Required for a Pilot to Respond to an Aircraft Disturbance," NASA TN D-221, Washington, DC, March 1960.

7. Ashkenas, I. L., & McRuer, D. T., "A Theory of Handling Qualities Derived from Pilot-Vehicle System Considerations," *Aerospace Engineering,* Vol. 21, no. 2, pp. 60–61,83–102, Feb. 1962.

8. Pedreiro, N., "Aplicação de um Modelo Matemático do Piloto Humano na Estimativa da Qualidade de Vôo" (Application of a Mathematical Model of the Human Pilot in the Estimation of Flight Qualities), M.S. Thesis, Instituto Tecnológico de Aeronáutica, São José dos Campos, Brazil, 1989 (in Portuguese).

9. Etkin, B., *Dynamics of Flight — Stability and Control,* 2nd ed., John Wiley & Sons, New York, 1982.

10. Howlett, J. J., "UH-60A Black Hawk Engineering Simulation Program: Volume I — Mathematical Model," NASA CR-166309, 1981.

11. Peters, D. A., & HaQuang, N., "Dynamic Inflow for Practical Applications," *Journal of the American Helicopter Society,* October 1988, pp. 64–68.

12. Mello, O. A. F., "Numerical Simulation of Helicopter / Ship Airwake Interactions," Progress Report submitted to Naval Air Warfare Center, School of Aerospace Engineering, Georgia Institute of Technology, Atlanta, December 1994.

13. Hoerner, S. F., "Fluid-Dynamic Drag," Published by the Author, 1965.